Charges at Aqueous Interfaces: Development of Computational Approaches in Direct Contact With Experiment

Robert Vácha

National Centre for Biomolecular Research, Faculty of Science and CEITEC - Central European Institute of Technology, Masaryk University, Kamenice 5, 625 00 Brno-Bohunice, Czech Republic

Frank Uhlig and Pavel Jungwirth

Institute of Organic Chemistry and Biochemistry, Academy of Sciences of the Czech Republic, Flemingovo nám. 2, 16610 Prague 6, Czech Republic

Corresponding authors: *robert.vacha@mail.muni.cz (RV) and pavel.jungwirth@uochb.cas.cz (PJ)*

CONTENTS

1. Introduction

Solutions of inorganic ions are ubiquitous in the natural and industrial environments, as well as in our bodies. While a lot of attention has been paid to the behavior of ions in bulk water since the late 19th century, there has been traditionally less emphasis on surfaces of aqueous electrolytes, despite their omnipresence in a wide range of processes in atmospheric chemistry, industrial technologies, and biochemistry (1-3). This may be partly due to the fact that classical theory describes water surface as essentially ion free due to the image charge repulsion (4-7). Such a view results from a continuum approximation of the interfaces as a contact between two homogeneous dielectrics with different permittivities (i.e., those of water and air), from which ions (represented mostly as point charges) are repelled. Around the turn of the millennium, computer simulations and surface sensitive experiments changed our view of ions at the surface of water (8-13). These results showed that the traditional picture of surface-depleted ions is a valid description only for small, non-polarizable (hard) ions, such as Na^+, K^+, or F^-. However, the situation is different for large soft, i.e., polarizable ions (I^-, SCN^-, and similar), which are found to be present at the surface of water.

The molecular mechanisms of surface behavior of inorganic ions are rather complex, involving both enthalpic and entropic contributions (14, 15). Different interactions have been invoked in explaining these mechanisms, which overcome the image charge electrostatic repulsion and bring ions to aqueous interfaces, including cavitation, polarization, dispersion, and surface potential effects. While all are clearly present, their relative importance remains to be a matter of debate. Dispersion is unlikely to be dominant and, when overemphasized, it wrongly sends hard rather than soft ions to the surface (16). The role of the surface potential due to preferential orientations of interfacial water molecules is a matter of intense discussions, where its most relevant

definition, as well as its size (or even sign) are only being established now (17-19).

The remaining two contributions, cavitation and polarization, are difficult to disentangle since, as a rule, the larger the ion the more polarizable it is (after all, polarizability is measured in volume units and characterizes the extent of the electron distribution of a given species). Also, there are different indications about the relative importance of polarization effects for surface propensities of ions. On one hand, surface propensities of ions yielding a satisfactory agreement with experimental measurables such as surface tensions can in some cases be obtained within non-polarizable force field simulations, implicitly accounting for certain polarization effects (20, 21). On the other hand, switching off polarization interactions in the simulations strongly reduces the affinity of ions for aqueous interfaces, which underlines the surface-stabilizing effects of both ion and water polarizabilities (9, 22-25).

There have been several recent reviews summarizing our knowledge about the behavior of ions at aqueous interfaces (21, 26-32). It is not our goal to rephrase here what has already been said in these publications. We are instead aiming at a relatively short review covering the most recent and/or controversial aspects of the field, not covered in the above reviews. The rest of the paper is organized as follows. In Section 2.1 we briefly describe technical problems connected with polarizable force fields stemming from the fact that polarization is an inherently many-body electronic effect, which can be only approximately accounted for using atomic polarizabilities and assuming a linear polarization response. For example, dampening of the polarization response leads to reduced ionic surface affinities, which points to the importance of proper treatment of polarization beyond linear response (33). A computationally cheap way how to completely circumvent such issues is to account for polarizability by an electronic continuum approach, which in practice means rescaling the ionic charges within a non-polarizable simulation framework (Section 2.2) (34, 35). A computationally

much more expensive approach is to move to *ab initio* molecular dynamics (AIMD), where polarization is consistently accounted for within an explicit electronic structure approach (Section 2.3) (36). In Section 3 we review two recent case studies of charged particles at aqueous interfaces, both of them accompanied with controversies. The first concerns the interfacial behavior of one of the inherent water ions - hydroxide (Section 3.1). The second is about the surface structure and energetics of the hydrated electron as a representative of a non-classical charged particle characterized by a soft (polarizable) electronic cloud (Section 3.2). In the spirit of a recent review on electrons and anions in water (37) we point to common features of the two cases and the roles of polarization and electron delocalization. We then close this review with a brief summary an attempt for qualified guess about developments in the field to be expected in the near future (Section 4).

2. Accounting for polarizability effects

2.1 Models with explicit polarization

In the most common implementations, polarization response is included via characteristics of individual atoms, i.e., atomic polarizabilities, Drude oscillators, or fluctuating charges, and its size increases linearly with the local electric field (38, 39). The induced dipole itself influences the electric field in the surrounding, which is why it is typically evaluated iteratively. This makes the simulations not only significantly slower, but also prone to a “polarization catastrophe”, when the induced fields are so large that the iterative procedure diverges (40, 41). This artifact originates from the linear relation between the induced dipole and the local electric field, which is valid only for small induced dipoles. This problem exists both in the point dipole and Drude oscillator implementations of the polarization response. The increased computer cost of a polarizable force field can be reduced by bypassing the above iterative procedure for

point dipoles by introducing an always stable predictor-corrector method (42) or by adding finite fictitious masses to the Drude particles (43).

Addition of polarizability to a non-polarizable force field does not make the model automatically better. It certainly provides additional degrees of freedom to fit. However, when added to the non-polarizable forcefield, caution should be exercised since the non-polarizable forcefield may effectively include some of the effects of polarizability already in the Lennard-Jones and electrostatic parameters. As a result, a polarizable model necessarily does not have to provide a better fit to experiment than a non-polarizable model. For example, the polarizable POL3 model (44) improves the properties of the non-polarizable TIP3P water (45), but it is comparable or even inferior to the non-polarizable SPC/E model (46) in several measurable properties, e.g., the melting point (47).

Over the last years a variety of corrections to the linear approximation to the polarization response, aimed at improving the account for polarizability and at preventing the polarization catastrophe, has been implemented. The simplest one is application of a size limit for the induced dipole, so that it can increase only up to a predefined maximum (48). More sophisticated linear and exponential screening function were also proposed and their performance is compared in a recent review (39). Another possibility is to add van der Waals parameters on the negatively charged Drude particle, which mimics the response of the electronic cloud to the electric field and the corresponding repulsive interactions at short distances (49). Finally, there is the possibility to add a dampening term for the electrostatic interactions at short distances (33). Apart from avoiding the polarization catastrophe the above implementations reduce the effects of polarizability, so that the surface affinity of ions such as iodide is lower than in simulations without the correction (33).

As the importance of polarizability in molecular simulations has been increasingly

recognized, new polarizable models of water and ions have been developed, some of which were parameterized with the focus on polarizability from the very beginning. For example the PD2-H2O point dipole model was specifically parameterized to reproduce polarizability in all spatial directions and its interactions with cations agree well with density functional theory calculations using the hybrid B3LYP functional (50). The SWM4-NDP (Simple Water Model with four sites and Negative Drude Polarizability), is a model developed as a part of the CHARMM force field for simulations of biomolecules (51). It is a reoptimized SWM4-DP model, where the Drude particle had a positive charge (52). The new model reproduces well the density, viscosity, diffusion, and hydration free energy of ambient liquid water. A new flexible polarizable model TTM3-F was introduced to the family of Thole-type water models with focus on reproducing the vibrational spectrum of liquid water (53). This is the third generation of a model parameterized against *ab initio* calculations that reproduces structural and energetic properties of water clusters and liquid water, where the partial charges are dependent on the geometry of the molecules. Even a more complex model is the ABEEM-7P fluctuating charges scheme (54) which is a part of the ABEEM force field (55). As the name suggest there are 7 point charges per water molecule – 3 for atoms, 2 for lone electron pairs, and 2 for bonds. The model, which was parameterized on the water dimer, yields ambient bulk permittivity of 76, which is close to to experimental value of 78, but also somewhat larger oxygen-oxygen distances than in the real liquid. A multipole water model has been introduced under the name DMIP (Distributed Multipoles Implicit Polarization) (56). It means that this model has permanent multipoles (up to quadrupoles) at atomic sites, where additional point dipoles can be induced. The model was fitted to *ab initio* calculations of small water clusters obtained from liquid bulk water simulated with the AMOEBA force field (57, 58). While accounting for polarization implicitly, properties of liquid water remained close to those of the AMOEBA force field

with a significantly reduced computer cost (56).

A simple and promising model (59) has been recently introduced to the existing family of polarizable waters (39, 60). The five-site POL4D model has negative charges located at two sites close to oxygen and the point dipole polarizability is located at oxygen atom (59). It has been shown that this model reproduces well the experimental water dipole, dielectric constant and viscosity, with the melting temperature estimated to be around 260 K. The value of the melting point is a common problem of water models that were parameterized for ambient conditions. As mentioned above, the point-dipole-based POL3 water model (44) has a significantly underestimated melting temperature of 180 K (47). Similarly, the SWM4-NDP model has melting temperature of 185 K (61). The *ab-initio*-based TTM3-F water model which melts at 250 K (53) and the POL4D model (59) are closest to reality, but still yield slightly lower melting points than the experimental value of 273.15 K. Another commonly underestimated feature in water models is the surface tension, which is important for interfaces.

New polarizable force fields have been developed not only for water but also for ions, building on older parameterizations (57, 62, 63). A novel parameterization for halide ions was derived based on high level *ab initio* calculations of small water clusters and/or employing the force matching procedure (64, 65). Water bulk simulations with the TCPEp water model resulted in diffusion coefficients and hydration of ions, which are in agreement with neutron and X-ray diffraction experiments (66). Applications of conventional polarizable force fields to simulations of ions at aqueous interfaces have been summarized in several reviews mentioned already in the Introduction (27, 28, 30). Recent developments including polarization dampening are discussed in the context of ionic surface propensities in Ref. (31). This study stresses that an accurate account for the polarization response is important for qualitative description of ions at aqueous

surfaces and that polarization dampening leads to reduced ionic surface affinities. Finally, we mention that complementary advances in parameterizations of non-polarizable force fields for ions with focus on aqueous surfaces are summed up in another recent review (21).

2.2 Implicit polarization via charge scaling

Is it possible to at least approximately account for polarization effects within the framework of non-polarizable force fields? Although this may sound almost like an oxymoron, let us have a closer look at the issue. The response of water molecules to dissolved charges has two components – nuclear reorientation and electronic polarization. The dielectric constant of water can thus be viewed as a product of two terms. The first one, which is due to reorientation of water molecules, is explicitly accounted for in non-polarizable simulations. The second one, which is related to induced shifts in electronic distributions of water molecules, is in principle missing from non-polarizable simulations. It is responsible for the electronic part of the dielectric constant, which for water equals to $\varepsilon_e = 1.78$ (67). Many non-polarizable water force fields, such as SPCE or TIP4P, account for this effect implicitly by increasing the static dipole of water from its gas phase value of 1.9 D close to (but not quite to) its bulk liquid value of about 2.9 D, yielding dielectric constants not far from, but typically lower than the experimental value of 80 (68).

The problem remains what to do with the insufficient dielectric screening to which ions are exposed in non-polarizable water. It can be easily shown that accounting for the electronic response of the solvent in a continuum dielectric fashion is mathematically equivalent to rescaling ionic charges by $\varepsilon_e^{-1/2}$ (34). Practically, this electronic continuum correction means running the non-polarizable simulation of aqueous salt solutions as usual, except with charges of the ions being reduced by 25 %. It has been shown

recently that this charge scaling, which has incidentally been used in simulations of ionic liquids as an effective fix (69), significantly improves agreement with experiment for ion pairing, particularly if polyvalent ions are present (34, 70).

The concept of scaling the charges of ions has been also employed to investigate their propensity for the air/water interface, albeit without connecting it to an implicit account for polarizability (15). Another issue is the discontinuity of electronic polarizability, which abruptly changes from 1.78 to 1 at the water/air interface. This means that the ionic charges are "overscaled" at the surface, since there should be no scaling in the gas phase with dielectric constant of about 1. As a result, the surface propensities of ions (see Figure 1) tend to be overestimated within this approach (35). Nevertheless, the effective account for polarizability should be well applicable for water/oil interfaces, which are practically continuous in terms of electronic polarizability (ε_e acquiring for oils values around 2). Indeed, our calculations employing this method yield ionic propensities for the water/oil interface (Figure 1) which are quantitatively comparable to results obtained from experiments and simulations with explicitly polarizable force fields (35).

2.3 Beyond conventional force fields

There is a need to go beyond conventional non-polarizable or polarizable force fields when the electronic structure changes significantly during the simulation, such as during chemical reactions or (partial) electron transfer processes. To the latter, allowing for a change of partial charges on atoms during the simulation can better mimic the transient behavior of the electronic wave function than a static description in the classical force filed. In the context of water simulations a charge-transfer model has been developed recently (71, 72). This model, parameterized against *ab initio* calculations for

the water dimer, allows for a small (about 0.02 e) transfer of the electronic charge along a water-water hydrogen bond. In the on average isotropic bulk environment such charge transfer can only occur transiently, but has to average out to zero. Simulations of the (inherently anisotropic) aqueous hydrophobic interfaces showed that in these cases there is a non-zero net charge profile perpendicular to the interface due to the charge transfer mechanism (73, 74). The local imbalance between hydrogen bond acceptors and donors resulted in a layer of a positive charge right around the Gibbs dividing surface (GDS) which, however, becomes overcompensated about 5 Å below the GDS, leading to a net negative charge in this region, which can be associated with the slip plane of the water/oil interface (73). The charge transfer mechanism can thus contribute to the zeta potentials observed in electrophoretic mobility measurements on aqueous oil emulsions or gas bubbles (73, 74), as discussed in more detail in Section 3.1.

Provided a change in bonding topology occurs in the simulation, such as during a chemical reaction or proton transfer in water, the Multi-State Empirical Valence Bond (MS-EVB) method can be used (75, 76). In this scheme a Hamiltonian matrix is composed of diagonal elements representing individual chemically distinct states and off-diagonal terms allowing for transitions between them. This method was applied to studies of proton transfer in water, including its interfacial behavior, yielding a strong surface enhancement of the hydronium cation (77, 78). Most recently, a polarizable version of the MS-EVB method was also used to investigate the surface behavior of the ionic product of water yielding practically flat free energy profiles (i.e., little surface enhancement) for either the hydronium cation or the hydroxide anion (79, 80).

A straightforward, albeit computationally very demanding way how to account for polarization effects is to describe the electronic structure of the system explicitly by molecular dynamics simulations with forces obtained using *ab initio* methods. Since the computational costs are immense, so far only density functional theory (DFT)

approaches in the generalized gradient approximation provided sufficiently efficient and accurate means for molecular dynamics simulations of extended interfacial aqueous systems (81). A first insight into the effect of polarizability on the surface propensities of large, polarizable ions, such as the nitrate ion and sulfate dianion, was gained from *ab initio* molecular dynamics (AIMD) simulations of medium-sized water clusters (82, 83). Both ions have a high polarizability, but differ significantly in their charge density. Whereas strong electrostatic interactions between the sulfate dianion and water lead to preferential interior solvation, propensity for surface solvation is observed for nitrate ions in small water clusters (82, 83). However, a caveat of molecular dynamics studies of cluster systems is an inherent bias toward surface solvation due to the high surface area to bulk volume ratio and surface curvature effects (84). Studies involving extended surfaces in slab geometries are thus needed to quantitatively elucidate propensities of ions for surface solvation. A computationally challenging factor is the minimal size of about 200 water molecules required to mimic faithfully the slab geometry, providing simultaneously well-behaved surfaces and a well-developed bulk phase (81). In recent years, AIMD simulations of different ionic solutes, such as hydroxide (36), hydronium (85), perchlorate (86), fluoride (87) and iodide (88) have been conducted, often in combination with the calculation of potentials of mean force in order to elucidate the surface affinities of these aqueous ions.

More specifically, AIMD simulations of a fluoride ion constrained at different distances from the interface of a 215 water molecule slab revealed that there are only minor differences between the solvation structure of the ion in the water bulk and at the water surface (87). As for the bulk ion solvation, dipole moments of interfacial water molecules increased when a fluoride anion was present near the GDS. The induced dipole moment of the fluoride anion increased upon moving closer to the water surface, but the relative change to the bulk value was small. In comparison, AIMD simulations of

an iodide anion in a water slab with a very similar computational setup and same system size showed a greater increase in the induced dipole moment of the anion upon moving from bulk to surface hydration (88). The obtained, rather flat potential of mean force for moving the iodide ion from the bulk to the water surface showed good correlation with results from a dielectric continuum theory, which accounted for cavitation effects and polarizability (24). This comparison underlines the importance of a proper treatment of electronic polarization.

In this context, it is worth mentioning that the AIMD potentials of mean force differ quantitatively, but not qualitatively, from results obtained using empirical polarizable force-fields (27, 28). All simulations exhibit a free energy minimum for an iodide ion solvated at the water-vapor interface. It is, however, less pronounced in the AIMD simulations, which suggests that the ionic surface affinity is overemphasized within a standard polarization treatment in the force field simulations (88). Nevertheless, qualitative trends for ionic surface propensities are the same. Both classical force field and AIMD simulation protocols suggest that large, polarizable ions have a stronger preference to accommodate at the interface than small, non-polarizable ions, which prefer bulk hydration (27, 28, 88). These effects are also related to the corresponding differences in solvation structures between strongly and weakly hydrated ions. In order to quantitatively understand the subtle effects involved an *ab initio* account of solute-solvent interactions is certainly favorable.

AIMD simulations with their many-electron treatment of electronic polarization effects start to represent a powerful and indispensable tool for explorations of ion-specific effects at the water/vapor interface. An non-classical example of a very polarizable charged solute in water is the hydrated electron. This crucial species for radiative processes in water has received significant attention since its discovery in the 1960s (89), but quantitative understanding of its bulk and surface solvation has been

only emerging recently (90-93) and several issues concerning its structure are still controversial (94-98). The investigation of the hydrated electron relies on quantum mechanical methods as a purely classical treatment is clearly out of question. While traditionally only the solvated electron has been treated quantum mechanically within pseudopotential approaches (90, 94, 99-103), AIMD description has become feasible recently (92, 93, 104-106). In Section 3.2 we present an AIMD study of the solvated electron at the water surface.

3. Case studies

3.1 Hydroxide at aqueous interfaces

There has been an ongoing controversy concerning the propensity of hydroxide to the surface of neat water. As far back as in 1861 migration of air bubbles toward the positive electrode was observed in water, pointing to their effective negative charge (107). This observation was followed by a series of experiments on water droplets in air flows or waterfalls, where a negative potential was measured in the proximity of droplets (108, 109). Early electrokinetic experiments on air bubbles were repeated and improved later, leading to similar results (110, 111). It was also shown that the negative charge on the bubbles or oil droplets around neutral pH can be titrated out at pH 3-4 (112-115). This is consistent with interpretations of the disjoining pressure measurements on thin aqueous films without surfactants, where negative charge at neutral pH was measured and isoelectric point was found to be also around pH 4 (116-118).

A relatively widespread interpretation of this phenomenon assumes surface adsorption of hydroxide ions as strong as 25 kT, leading to an estimated surface charge of about -5 μC/cm^2 (i.e., about one OH^- per 3 nm^2 of the surface) at neutral pH (113-115, 119, 120). However, this interpretation is in conflict with surface and molecular selective spectroscopic techniques such as second harmonic generation (SHG) (121) and

photoelectron spectroscopy (PES) (122, 123), which ruled out strong hydroxide adsorption. Similarly, recent sum frequency generation (SFG) measurements do not show any surface adsorption of hydroxide (73), which also calls for reinterpretation of earlier SFG experiments (124). Moreover, such a strong OH^- adsorption would be incompatible with the increase of surface tension of water upon adding hydroxide (125, 126). Recent attempts to focus on the dynamic surface tension (127) miss the point that the Gibbs adsorption equation cannot be violated (128), moreover, the dynamic effects on surface tension have been rationalized in terms of surface cooling more than three decades ago (129).

Computer simulations ranging from large water clusters to extended aqueous interfaces show consistently no appreciable adsorption of hydroxide at the water surface. More specifically, *ab initio* calculations demonstrated asymmetric solvation of OH^- in very small water clusters (130, 131) which, however, becomes diminished in larger clusters (132-134). Polarizable molecular dynamics simulations of extended aqueous slabs showed a very weak repulsion of hydroxide from the water surface, such that it can still be present (but not enhanced) at the interface (79, 134, 135). Similarly, an *ab initio* molecular dynamics simulation of 215 water molecules arranged in slab geometry showed a negligible (below ~kT) affinity of hydroxide toward the water surface (36). An analogous OH^- behavior was reported for other water/hydrophobic interfaces (e.g. the water/oil interface) (136), with the exception of a rigid hydrophobic interface, where a somewhat stronger hydroxide adsorption was observed due to interfacial water structuring (136-139), as shown on Figure 2. Given the various potential inaccuracies of the different computational approaches, it is rather remarkable what a consistent picture, which excludes strong adsorption of hydroxide to water surface, the simulations provide.

During the last few years, the apparent controversy between spectroscopic and simulation data showing little surface affinity of hydroxide and the interpretation of

electrophoretic and titration experiments in terms of a dramatic surface adsorption of OH^- has been raised and discussed (122, 140-144). Note that the macroscopic measurements only show a presence of an apparent and titratable negative charge at aqueous interfaces, but do not reveal its chemical nature. In an attempt to provide an explanation consistent with the spectroscopic and simulation evidence, we have recently explored the potential effects of charge transfer between water molecules using models described in Section 2.1 (73, 74). We have indeed shown that the anisotropy of water hydrogen bond distribution at the interface results in a region of a net negative charge at around 5 Å below the GDS (73, 74), see Figure 3. Estimates based on a continuum water model indicate that the zeta potential originating from this charge transfer has the right negative sign, but its value of roughly -2 mV is about an order of magnitude smaller that measured in electrophoretic mobility measurements (74).

In the context of the existing controversy the most recent study on the mobility of oil droplets in aqueous emulsions made of 99 % or 99.8 % pure hexadecane should be mentioned (145). The authors of this study demonstrated that the large negative zeta potential of droplets made out of less pure 99 % hexadecane is due to the presence of titratable impurities, since the effect all but disappears in the purer oil. Moreover, the reported pH dependent zeta potential curve can be restored by adding a small amount of fatty acids to the purer oil (145). The resolution of the controversy in terms of traces of fatty acids has been criticized almost immediately (146, 147) and it remains an open question to what extent the data reported in the literature are due to impurities. Time will tell, but already now we can put the following constraints on a physically acceptable interpretation of the observed phenomena: It should not violate basic thermodynamics, such as the Gibbs adsorption equation and it should not enforce a species to be at the same time a strongly soluble one (solubility of NaOH is about 1 kg/1 l of water) and an extreme surfactant, since these two features are mutually exclusive. It should also

respect the fact that spectroscopic techniques which are ion-specific do not provide evidence for accumulation of hydroxide at the water surface. As a final remark, when referring to hydroxide or hydronium at the surface of water, the terms “basic” (119, 148) or “acidic” (134, 135, 149) should be used with caution and only in quotation marks, since strictly speaking they do not refer to surface concentration but to surface activity of these ions (122). At thermodynamic equilibrium a chemical potential of an ion is constant throughout the sample, therefore, a pH neutral bulk water has also a pH neutral surface, despite the fact that the surface concentrations of hydronium and hydroxide can differ from those in the bulk.

3.2 Solvated electron at the surface of water

Despite its non-classical nature, a poster child for polarizable charged species in water is the so-called hydrated electron (89). On one hand, it can be viewed as the most simple charge in water, since the hydrated electron emerges upon the localization of a single (excess) electron in water, e.g., after photoionization or radiolysis of water or salt solutions (150, 151). On the other hand, due to the quantum mechanical nature of the electron it is difficult to disentangle the whole system into distinct parts, i.e., the excess electron and the aqueous solvent. The high flexibility (i.e., softness or polarizability) of the hydrated electron compared to ions arises to a large degree from the absence of an associated nucleus and the corresponding core-electron attraction.

Due to the explicit quantum nature of the hydrated electron, theoretical modeling is posed with serious challenges. Two different approaches are commonly employed for molecular dynamics investigations. Forces on the nuclei are obtained either from a full quantum mechanical treatment of all (valence) electrons of surrounding water molecules or employing an artificial split between the excess electron and the rest of system.

Within the latter, only the excess electron is treated quantum mechanically, while the interactions with the remaining part of the system are cast into a pseudopotential with water molecules being treated within a classical force field. The pseudopotential approaches have found a widespread use because of their computational efficiency, but they rely heavily on their parameterization. Apart from a recent controversy about a particular pseudopotential parameterization yielding a very delocalized electron (94-97), the consensus about the structure of the hydrated electron in bulk water has been that of a charge primarily localized in a cavity formed by about four water molecules (90, 103). Our most recent AIMD simulations provide, however, a more complex picture of the hydrated electron, where the cavity is indeed the leading motif, but the delocalized part and the overlap with surrounding water molecules account together for more than 50 % of the electron density (93).

The picture of an electron at the surface of water has been less clear. Already from the beginning of pseudopotential calculations, quantum path integral dynamics (QUPID) simulations showed that an excess electron can bind to cold (79 K) water clusters either in an interior, cavity-like state or at the surface of the cluster, the latter states being more diffuse and lower in binding energy (152). From further QUPID simulations of larger water clusters (with up to 128 molecules) at higher temperatures it was speculated that a transition from surface-bound to interior-bound isomers would occur for clusters comprising more than about 64 water molecules. This conjecture was based on the relative vertical binding energies of an hydrated electron at the exterior and interior of water clusters (99). A similar observation was made from molecular dynamics of even large water clusters (up to 8000 molecules) using a different pseudopotential model (153). While the electron was stable both at the surface and in the interior of the clusters at 200 K, a transition to interior states occurred for large clusters at 300 K. Related findings from photoelectron spectroscopic measurements of cold anionic water

cluster of varying sizes confirmed the existence of different isomers for each cluster size that extrapolate to different values for infinite systems (154, 155). While the strongly bound isomer (isomer I) can represent interior or surface bound states, there is a general consensus that the more weakly bound state (isomer II) is a surface isomer (101, 154, 156). Both on theoretical (101, 156) and experimental (155) grounds, it was argued that isomer II represents a metastable, kinetically trapped state on cryogenic clusters that would not be present under ambient conditions. It was also noted, that the localization mode (interior vs. surface) of an electron to water clusters strongly depends on the thermal history of the cluster before electron attachment (156-158).

A drawback of most of the pseudopotential calculations is the lack of mutual polarization between the excess electron and the water molecules and also between the water molecules themselves. Recently it was acknowledged by two independent pseudopotential implementations that the inclusion of mutual many-body polarization of the excess electron wavefunction with the surrounding water molecules leads to improved results for structure, energetics, vertical binding energy (VDE) and optical absorption spectrum in bulk water as well as for anionic water clusters (159, 160). The former pseudopotential was also tested on water clusters in the range of 20 to 200 water molecules and several distinct surface isomers could be observed. From these, only strongly bound isomers are persistent in dynamics at 200 K, when considerable rearrangements of the molecular framework become accessible. It was observed that structures with the excess electron partially embedded at the cluster surface or bound in an interior cavity-like structure extrapolate to the same limiting value for infinite cluster size (albeit with a slightly different slope) when the VDE is plotted against the inverse linear size of the cluster. These findings are in good agreement with previous observations that the isomer I might consist of different structures that can only be detected at very high resolution (155). Also, assignment by pseudopotential calculations

suggested that isomer I may correspond to a surface-bound structure (101). Finally, AIMD simulations of large anionic water clusters showed only marginal differences in VDEs for surface- and interior-bound hydrated electrons at ambient conditions (156, 161).

Summarizing the above findings, it is becoming apparent that the different binding motifs found in anionic water clusters are merely remnants of the kinetic trapping of hydrated electrons in diffuse structures at the cluster interface at very low temperatures and that at ambient conditions a hydrated electron at the surface and in the interior of a large water cluster are likely to be very similar in structure and energetics. This is in line with our recent findings from ab initio molecular dynamics simulations employing a coupled quantum mechanics/molecular mechanics (QM/MM) approach to extended systems at ambient conditions (93, 162). Namely, simulations of a hydrated electron in bulk water and at the water/vapor interface were performed and a striking similarity between the two systems was found (93, 162).

In Figure 4 the hydrated electron at the surface and in the bulk is depicted together with the surrounding water molecules. Already from this visual inspection the similarity between bulk and surface solvation is apparent, with the excess electron being submerged in the first surface layer of the water/vapor interface and thus practically completely retaining its first solvent shell. This is consistent with recent SHG measurements, which showed that an electron at the surface of water is not disturbed by surfactants which do not penetrate into the first water layer, but its properties change upon addition of surface-penetrating amphiphilic molecules (163). A more quantitive analysis yields the decomposition of the hydrated electron density into an interior cavity, overlap with water molecules, a diffuse interstitial part and (in the case of the interface) the part protruding in the vapor phase. In Figure 5 we show the corresponding decompositions of the spin density for both bulk and surface hydrated electron. All

contributions are very similar to each other at the surface and in the bulk, with the interior cavity containing 37 % (surface) and 40 % (bulk) of the hydrated electron. At the surface both the diffuse part and the overlap with water molecules are slightly reduced compared to bulk solvation. This is due to the anisotropy of the water/vapor interface, nevertheless, the first solvent shell does not change upon surface solvation and appreciable differences arise only in the second solvent shell around the hydrated electron.

The solvation structure of water around the hydrated electron can be characterized by radial distribution functions (RDFs), which give a measure of the statistical distribution of one species around another compared to an ideal gas distribution. The RDF for oxygen atoms around the center of the hydrated electron is shown in Figure 6. An enhancement of water molecules around the hydrated electron can be seen from the peak at around 2.5 Å. About four water molecules contribute on average to the first solvation shell. We can (artificially) split the RDF into the contributions of single oxygen atoms (colored lines in Figure 6). It is worth noting that already over the 10 ps duration of the simulation exchange of water molecules in the first solvent shell already occurred, indicating that the solvent cage around the hydrated electron is rather flexible.

In a similar spirit to the above split of the RDF, we can decompose the (vibrational) spectral density of water molecules in the system into contributions from molecules close to the electron and the remaining water molecules. The spectral density for the QM water molecules in the first solvent shell of the surface solvated electron, obtained as a Fourier transform of the velocity autocorrelation function, is shown in blue in Figure 7. The dangling OH peak at roughly 3650 cm^{-1}, which is missing for the bulk solvated electron, demonstrates that at least one water molecule close to the electron is directly located at the water/vapor interface. Furthermore, red-shifts for both bending and

librational motions are observed in proximity to the hydrated electron, which correlates well with experimental observations in water clusters (164, 165).

It is crucial to check the robustness of the above results with respect to the electronic structure methods used. In our previous studies it was shown that comparable results for the hydrated electron in medium-sized water clusters can be achieved using different density functionals (namely PBE or BLYP) (166) and also that for small clusters a very good agreement between RI-MP2 and self-interaction corrected DFT methods can be achieved for structure and reactivity of the hydrated electron in small protonated water clusters (167). An important factor determining quality of the calculations is the basis set. In all presented calculations a sufficiently flexible atom-centered basis set was augmented by an additional auxiliary basis set of Gaussian functions, which spread regularly in space spherically surrounding the center of the hydrated electron (93). Within the QM/MM approach care has to be taken that this grid of functions does not spread over the boundaries implied by the QM atoms, otherwise artificial spill-out effects into the MM part can occur. In Figure 8 we compare the correlated distributions of radii of gyration and VDEs for two different setups for the bulk hydrated electron. The first setup employs a grid of 19 additional auxiliary basis functions in a QM/MM system with 32 QM and 992 MM waters, while the second setup employs 64 QM and 960 MM water molecules and a larger grid of 81 auxiliary functions. The range and distributions of vertical detachment energies are very similar in both simulations, with the hydrated electron's radius of gyration being only slightly larger (by about 0.1 Å) on average for the system with more QM molecules and the larger basis set.

From the simulations, it is evident that not only in bulk liquid water but also at the water/vapor interface the hydrated electron behaves as a (practically) fully solvated charged species, similarly to ions (168). This is in stark contrast to the situation in cryogenic solid state clusters where diffuse and weakly bound isomers of the electron

can be kinetically trapped (154). Interestingly, the first PES study of electrons in liquid microjets suggested, based on extrapolations from cryogenic clusters, such a weakly bound surface structure (with VDE of 1.6 eV) also for liquid water (98, 169). In contrast and, at the same time, in line with calculations, later PES measurements in liquid microjets, performed at somewhat different experimental conditions, found only strongly bound (VDEs of 3.2 – 3.7 eV) hydrated electrons (170-172).

Outlook

The goal of the present paper has been to address issues connected with affinities of ions and electrons to aqueous interfaces with emphasis on polarization as an important driving force for the observed effects. Proper account for polarization interactions represents a significant challenge for force field based simulations. Approaches based on a linear relation between the electric field and the polarization response tend to overestimate polarization effects. As a consequence, these calculations typically yield stronger surface excesses of soft ions then deduced, e.g., from surface tension measurements. One way to correct for this is to dampen the polarization response, while other approaches are based on accounting for polarization in an effective way via scaling of ionic charges or by models including charge transfer. *Ab initio* molecular dynamics is in the meanwhile becoming a possible method of choice, despite its significant computational costs, since it consistently and without potential force field bias accounts for electronic interactions including polarization. This approach, when properly benchmarked, should eventually allow for a quantitative assessment of the relative importance of polarizability with respect to other factors, such as the surface potential and entropic contributions, for the surface propensities of soft ions.

As illustrations of the above computational approaches we have discussed two experimentally relevant and controversial studies, namely the surface behavior of the

hydroxide ion and the hydrated electron. In each of the two cases, a peculiar interfacial behavior has been inferred from some measurements. OH^- has been postulated to be an extremely strong surfactant and a weakly bound delocalized surface structure has been suggested for the hydrated electron. We have shown that in neither case is such a surface behavior in line with molecular simulations and spectroscopic experiments, nor is it consistent with thermodynamic requirements. The picture emerging from our studies, which certainly needs a more detailed future examination and validation, is that both polarizable inorganic anions and electrons behave in many respects very similarly in the bulk and at aqueous interfaces. This is because at the surface these charged species do not become “half-dehydrated”, as one could naively expect, but rather maintain most of their bulk hydration structure and properties.

Figure captions:

Figure 1: Density profiles from simulations with scaled ionic charges of ions at the water/air and water/oil interfaces. Ion densities are scaled by the water/ion concentration ratio of 55.56 and the Gibbs dividing surface for water is taken as the origin of the x-coordinate in all cases.

Figure 2: Density profiles of hydroxide (red), water (blue), and the hydrophobic phase (black). Note the weak repulsion of OH^- from the interface ((a), (b), and (d)), except for the case of the hydrophobic wall (c), where a weak attraction is observed.

Figure 3: Hydrogen bond balance profiles (blue) and charge profiles (red) at the water-vapor and water-oil interfaces. The profiles are depicted as dashed lines, while integrals thereof, i.e., cumulative profiles are shown as full lines. Note the region of cumulative negative charge around 5 Å below the Gibbs dividing surface.

Figure 4: Snapshot of the hydrated electron at the water/vapor interface (A) and in the aqueous bulk (B). Isosurfaces of the spin density at 0.001 and 0.0001 $Bohr^{-3}$, encompassing roughly 70 and 90 % of the hydrated electron. Water molecules are in licorice representation, QM atoms opaque and thick and MM atoms transparent and thin.

Figure 5: Radial profiles of the hydrated electron in water bulk (black, dashed lines) and at the air/water interface (black, full lines). The cavity contribution is shown in blue, part of the hydrated electron on water in red and diffuse part in magenta. Surface contribution in green (only present at the air/water interface).

Figure 6: Radial distribution function of oxygen atoms around the center of the hydrated electron (black line) and radial distribution functions of individual oxygen

atoms that show significant contribution to the first solvation shell at some point during the molecular dynamics (colored).

Figure 7: Power spectral density of the QM atoms in the simulations of a surface hydrated electron (red line). The full, blue line shows the same for the water molecules in the proximity of the hydrated electron and the green line the remaining part. The inset depicts the power spectral density in the OH stretching region for the QM atoms close to the hydrated electron. Full line - water molecules at the surface and dashed line – water molecules from the bulk simulation.

Figure 8: Correlated distribution of vertical detachment energies and radii of gyration for two different system size setups. Both simulations consisted of 1024 water molecules in total, for blue 32 water molecules were treated as QM and for green 64. Additonally, the auxiliary grid of basis functions was increased when going to the system with more QM atoms.

Figures:

Figure 1

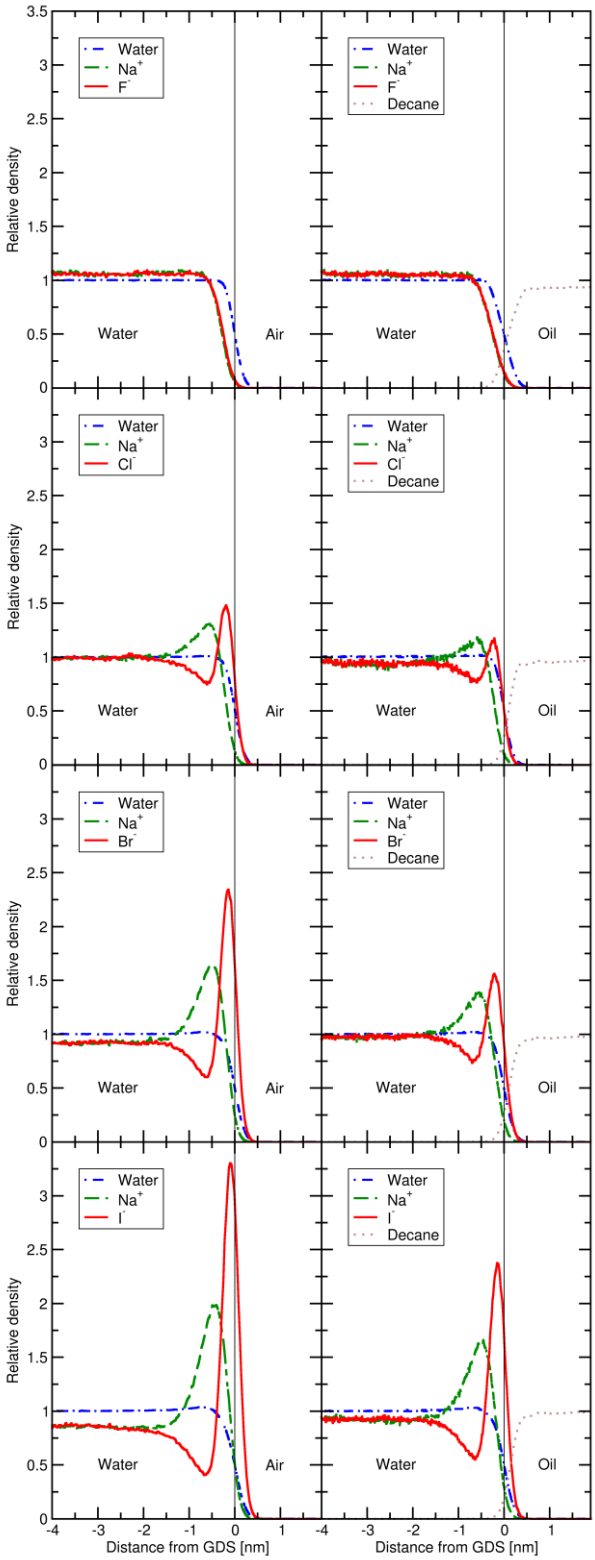

Figure 2

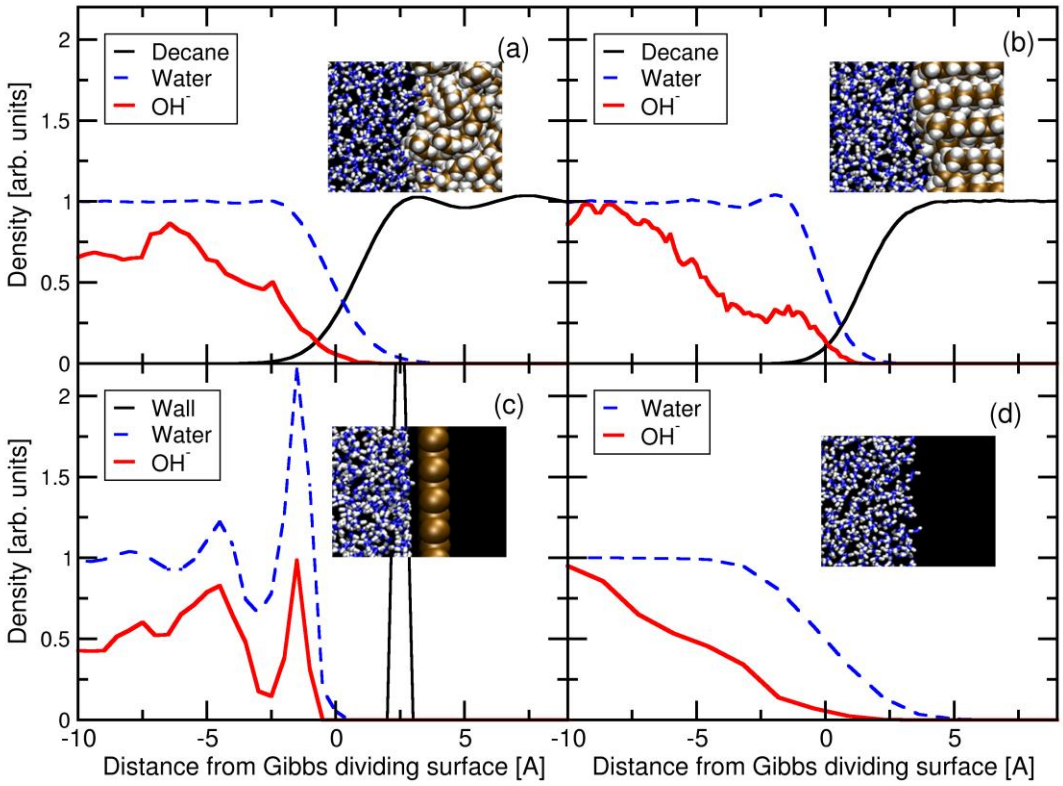
Decane
Water
OH-
(a)
(b)
Wall
Water
OH-
(c)
Water
OH-
(d)
Density [arb. units]
Distance from Gibbs dividing surface [A]
Distance from Gibbs dividing surface [A]

Figure 3

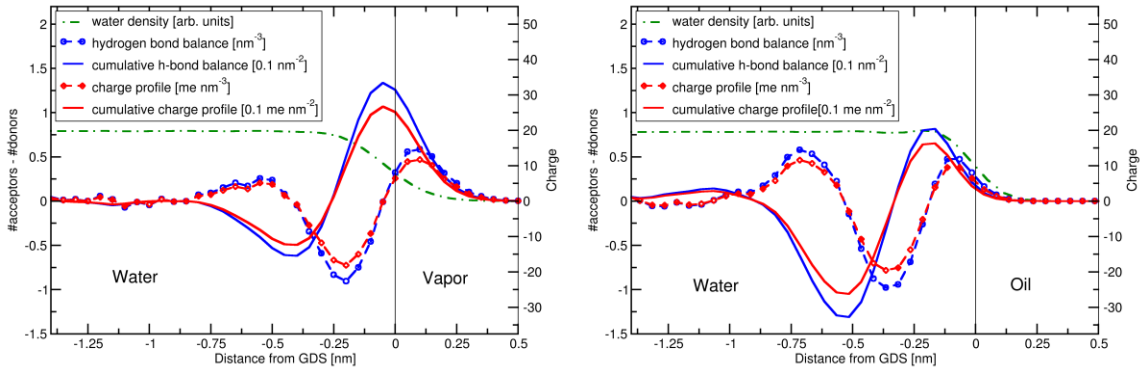
water density [arb. units]
hydrogen bond balance [nm-3]
cumulative h-bond balance [0.1 nm-2]
charge profile [me nm-3]
cumulative charge profile [0.1 me nm-2]
#acceptors - #donors
Charge
Water
Vapor
Distance from GDS [nm]
water density [arb. units]
hydrogen bond balance [nm-3]
cumulative h-bond balance [0.1 nm-2]
charge profile [me nm-3]
cumulative charge profile[0.1 me nm-2]
#acceptors - #donors
Charge
Water
Oil
Distance from GDS [nm]

Figure 4

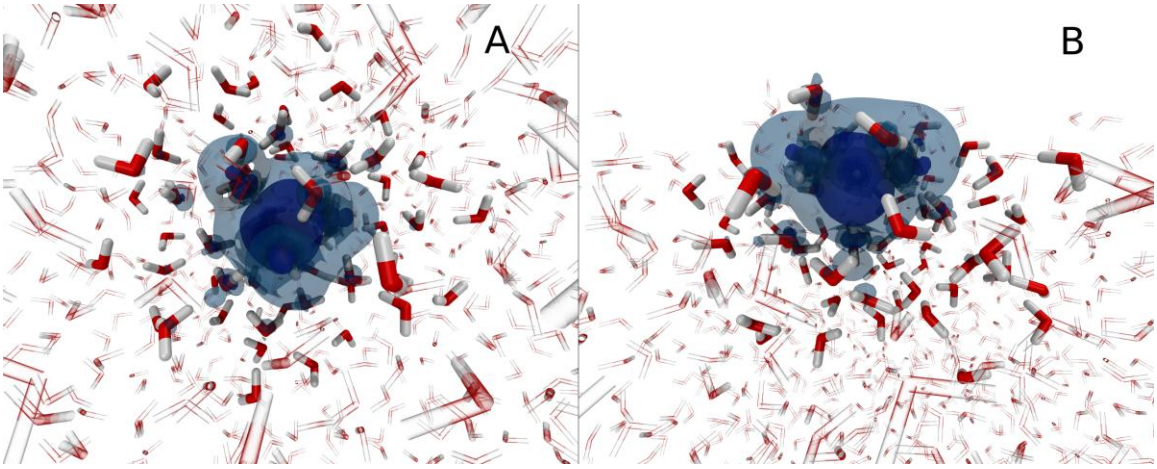

Figure 5

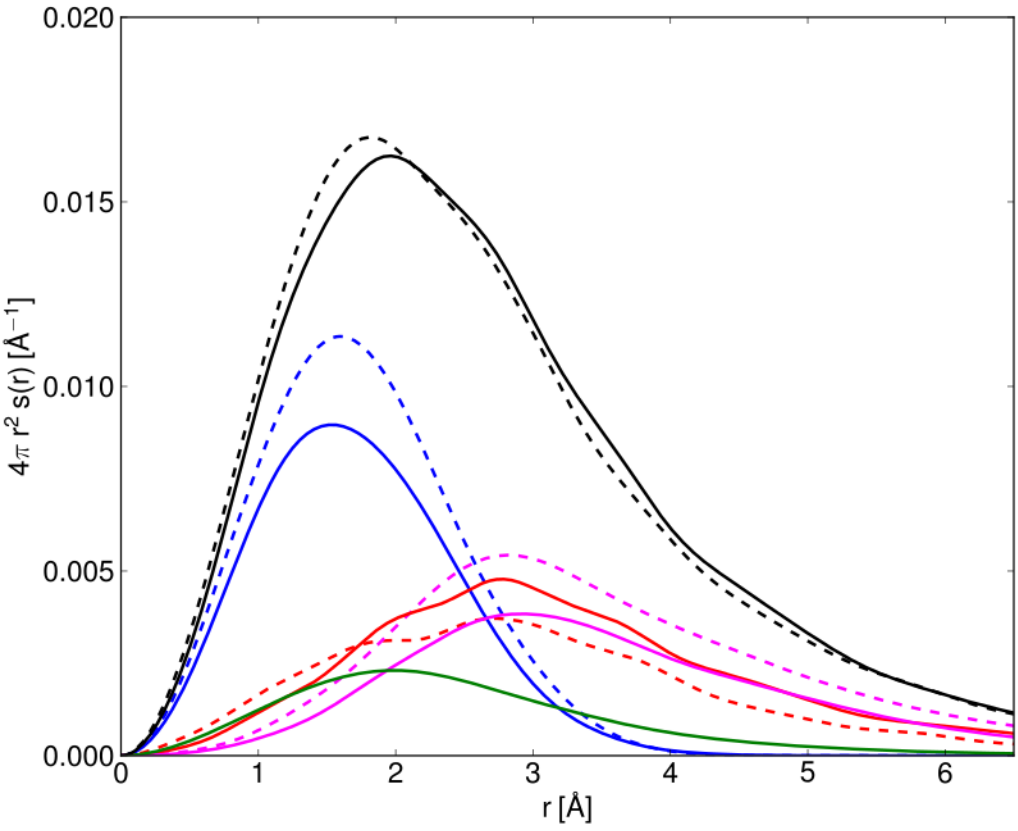

Figure 6

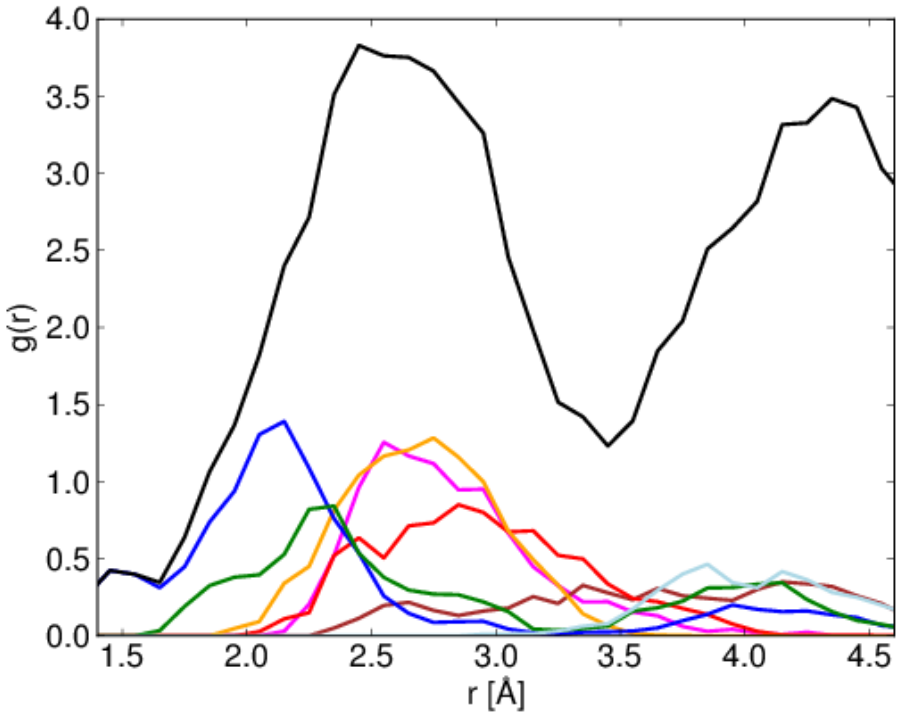

Figure 7

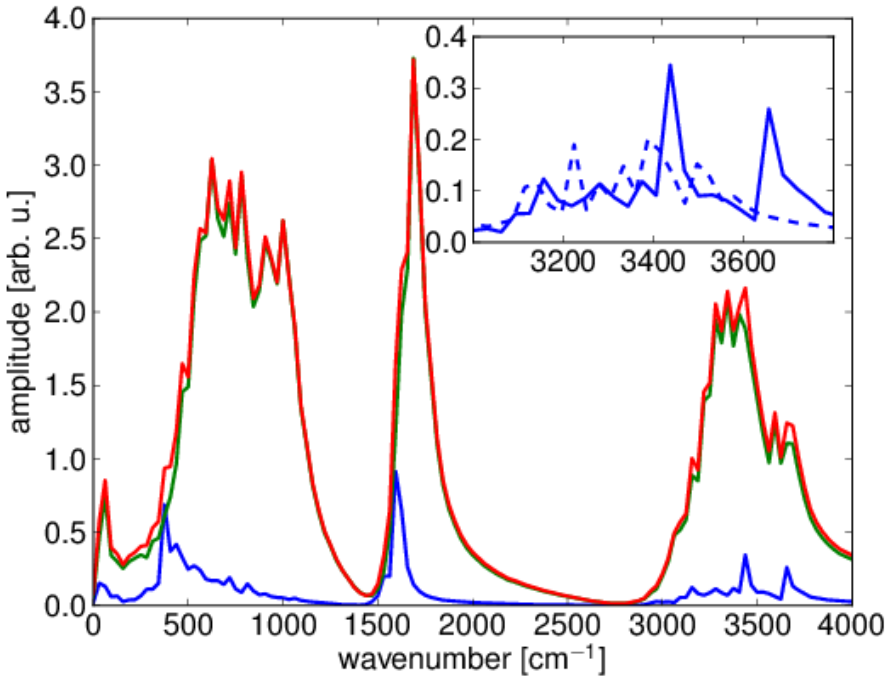
amplitude [arb. u.]
wavenumber [cm^{-1}]
0.0
0.5
1.0
1.5
2.0
2.5
3.0
3.5
4.0
0
500
1000
1500
2000
2500
3000
3500
4000
0.0
0.1
0.2
0.3
0.4
3200
3400
3600

Figure 8

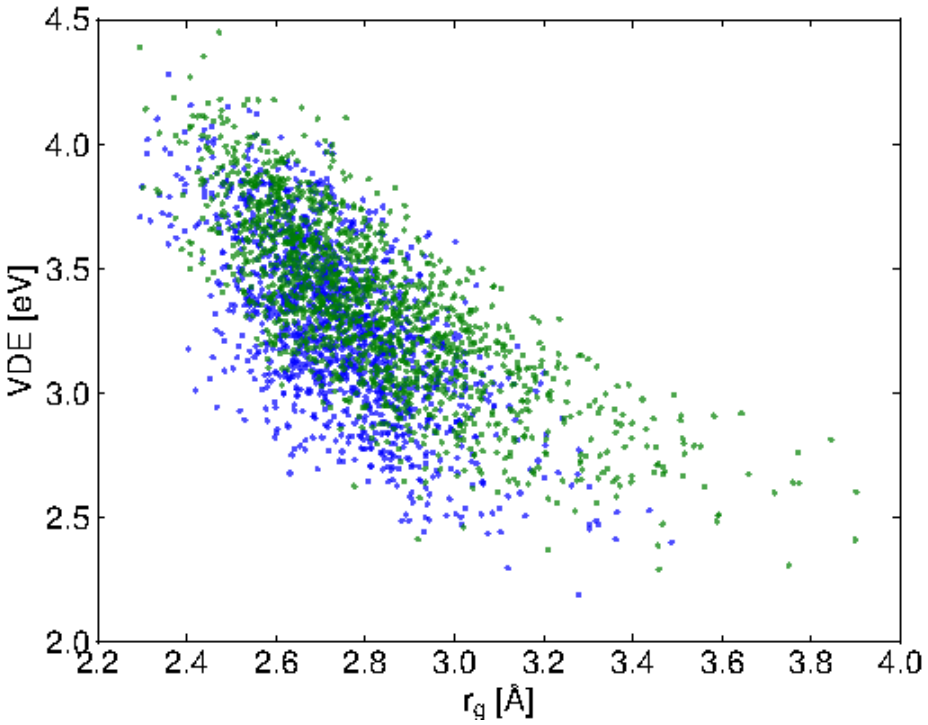

References

1. Finlayson-Pitts BJ (2003) *Chemical Reviews* **103,** 4801-4822.
2. Kritzer P (2004) *Journal of Supercritical Fluids* **29,** 1-29.
3. Zhang YJ & Cremer PS (2006) *Current Opinion in Chemical Biology* **10,** 658-663.
4. Onsager L & Samaras NNT (1934) *Jornal of Chemical Physics* **2,** 528-536.
5. Adam NK (1941) *The Physics and Chemistry of Surfaces* (Oxford University Press, London).
6. Randles JEB (1957) *Discussions of the Faraday Society***,** 194-199.
7. Randles JEB (1977) *Phys. Chem. Liq.* **7,** 107.
8. Jungwirth P & Tobias DJ (2001) *Journal of Physical Chemistry B* **105,** 10468-10472.
9. Dang LX & Chang TM (2002) *Journal of Physical Chemistry B* **106,** 235-238.
10. Liu DF, Ma G, Levering LM, & Allen HC (2004) *Journal of Physical Chemistry B* **108,** 2252-2260.
11. Raymond EA & Richmond GL (2004) *Journal of Physical Chemistry B* **108,** 5051-5059.
12. Petersen PB & Saykally RJ (2004) *Chemical Physics Letters* **397,** 51-55.
13. Ghosal S, Hemminger JC, Bluhm H, Mun BS, Hebenstreit ELD, Ketteler G, Ogletree DF, Requejo FG, & Salmeron M (2005) *Science* **307,** 563-566.
14. Caleman C, Hub JS, van Maaren PJ, & van der Spoel D (2011) *Proceedings of the National Academy of Sciences of the United States of America* **108,** 6838-

6842.

15. Otten DE, Shaffer PR, Geissler PL, & Saykally RJ (2012) *Proceedings of the National Academy of Sciences of the United States of America* **109,** 701-705.
16. Bostrom M, Williams DRM, & Ninham BW (2001) *Langmuir* **17,** 4475-4478.
17. Paluch M (2000) *Advances in Colloid and Interface Science* **84,** 27-45.
18. Kathmann SM, Kuo IFW, Mundy CJ, & Schenter GK (2011) *Journal of Physical Chemistry B* **115,** 4369-4377.
19. Baer MD, Stern AC, Levin Y, Tobias DJ, & Mundy CJ (2012) *Journal of Physical Chemistry Letters* **3,** 1565-1570.
20. Horinek D, Herz A, Vrbka L, Sedlmeier F, Mamatkulov SI, & Netz RR (2009) *Chemical Physics Letters* **479,** 173-183.
21. Netz RR & Horinek D (2012) in *Annual Review of Physical Chemistry, Vol 63*, eds. Johnson MA & Martinez TJ, pp. 401-418.
22. Vrbka L, Mucha M, Minofar B, Jungwirth P, Brown EC, & Tobias DJ (2004) *Current Opinion in Colloid & Interface Science* **9,** 67-73.
23. Archontis G & Leontidis E (2006) *Chemical Physics Letters* **420,** 199-203.
24. Levin Y, dos Santos AP, & Diehl A (2009) *Physical Review Letters* **103**.
25. Yagasaki T, Saito S, & Ohmine I (2010) *Journal of Physical Chemistry A* **114,** 12573-12584.
26. Gopalakrishnan S, Liu DF, Allen HC, Kuo M, & Shultz MJ (2006) *Chemical Reviews* **106,** 1155-1175.
27. Jungwirth P & Tobias DJ (2006) *Chemical Reviews* **106,** 1259-1281.
28. Chang TM & Dang LX (2006) *Chemical Reviews* **106,** 1305-1322.

29. Petersen PB & Saykally RJ (2006) *Annual Review of Physical Chemistry* **57,** 333-364.

30. Jungwirth P & Winter B (2008) *Annual Review of Physical Chemistry* **59,** 343-366.

31. Wick CD & Cummings OT (2011) *Chemical Physics Letters* **513,** 161-166.

32. dos Santos AP & Levin Y (2012) *Langmuir* **28,** 1304-1308.

33. Wick CD (2009) *Journal of Chemical Physics* **131**.

34. Leontyev I & Stuchebrukhov A (2011) *Physical Chemistry Chemical Physics* **13,** 2613-2626.

35. Vazdar M, Pluharova E, Mason PE, Vacha R, & P. J (2012) *Journal of Physical Chemistry Letters* **3,** 2087-2091.

36. Mundy CJ, Kuo IFW, Tuckerman ME, Lee HS, & Tobias DJ (2009) *Chemical Physics Letters* **481,** 2-8.

37. Ben-Amotz D (2011) *Journal of Physical Chemistry Letters* **2,** 1216-1222.

38. Lopes PEM, Roux B, & MacKerell AD (2009) *Theoretical Chemistry Accounts* **124,** 11-28.

39. Cieplak P, Dupradeau FY, Duan Y, & Wang JM (2009) *Journal of Physics-Condensed Matter* **21**.

40. Thole BT (1981) *Chemical Physics* **59,** 341-350.

41. van Duijnen PT & Swart M (1998) *Journal of Physical Chemistry A* **102,** 2399-2407.

42. Kolafa J (2005) *Journal of Chemical Physics* **122**.

43. Anisimov VM, Lamoureux G, Vorobyov IV, Huang N, Roux B, & MacKerell AD

(2005) *Journal of Chemical Theory and Computation* **1,** 153-168.

44. Caldwell JW & Kollman PA (1995) *Journal of Physical Chemistry* **99,** 6208-6219.

45. Jorgensen WL, Chandrasekhar J, Madura JD, Impey RW, & Klein ML (1983) *Journal of Chemical Physics* **79,** 926-935.

46. Berendsen HJC, Grigera JR, & Straatsma TP (1987) *Journal of Physical Chemistry* **91,** 6269-6271.

47. Muchova E, Gladich I, Picaud S, Hoang PNM, & Roeselova M (2011) *Journal of Physical Chemistry A* **115,** 5973-5982.

48. Petersen PB, Saykally RJ, Mucha M, & Jungwirth P (2005) *Journal of Physical Chemistry B* **109,** 10915-10921.

49. van Maaren PJ & van der Spoel D (2001) *Journal of Physical Chemistry B* **105,** 2618-2626.

50. Masia M, Probst M, & Rey R (2004) *Journal of Chemical Physics* **121,** 7362-7378.

51. Zhu X, Lopes PEM, & MacKerell AD (2012) *Wiley Interdisciplinary Reviews-Computational Molecular Science* **2,** 167-185.

52. Lamoureux G, MacKerell AD, & Roux B (2003) *Journal of Chemical Physics* **119,** 5185-5197.

53. Fanourgakis GS & Xantheas SS (2008) *Journal of Chemical Physics* **128**.

54. Yang ZZ, Wu Y, & Zhao DX (2004) *Journal of Chemical Physics* **120,** 2541-2557.

55. Zhao DX, Liu C, Wang FF, Yu CY, Gong LD, Liu SB, & Yang ZZ (2010) *Journal of*

Chemical Theory and Computation **6,** 795-804.

56. Walsh TR & Liang T (2009) *Journal of Computational Chemistry* **30,** 893-899.

57. Ren PY & Ponder JW (2003) *Journal of Physical Chemistry B* **107,** 5933-5947.

58. Ponder JW, Wu CJ, Ren PY, Pande VS, Chodera JD, Schnieders MJ, Haque I, Mobley DL, Lambrecht DS, DiStasio RA*, et al.* (2010) *Journal of Physical Chemistry B* **114,** 2549-2564.

59. Viererblova L & Kolafa J (2011) *Physical Chemistry Chemical Physics* **13,** 19925-19935.

60. Wang J, Cieplak P, Cai Q, Hsieh MJ, Wang JM, Duan Y, & Luo R (2012) *Journal of Physical Chemistry B* **116,** 7999-8008.

61. Lamoureux G, Harder E, Vorobyov IV, Roux B, & MacKerell AD (2006) *Chemical Physics Letters* **418,** 245-249.

62. Dang LX, Rice JE, Caldwell J, & Kollman PA (1991) *Journal of the American Chemical Society* **113,** 2481-2486.

63. Masia M, Probst M, & Rey R (2005) *Journal of Chemical Physics* **123**.

64. Trumm M, Martinez YOG, Real F, Masella M, Vallet V, & Schimmelpfennig B (2012) *Journal of Chemical Physics* **136**.

65. Spangberg D, Guardia E, & Masia M (2012) *Computational and Theoretical Chemistry* **982,** 58-65.

66. Masella M & Cuniasse P (2003) *Journal of Chemical Physics* **119,** 1866-1873.

67. Leontyev IV & Stuchebrukhov AA (2010) *Journal of Chemical Theory and Computation* **6,** 3153-3161.

68. Vega C & Abascal JLF (2011) *Physical Chemistry Chemical Physics* **13,** 19663-

19688.

69. Schroder C (2012) *Physical Chemistry Chemical Physics* **14,** 3089-3102.

70. Mason PE, Wernersson E, & Jungwirth P (2012) *Journal of Physical Chemistry B* **116,** 8145-8153.

71. Lee AJ & Rick SW (2011) *Journal of Chemical Physics* **134**.

72. Wick CD, Lee AJ, & Rick SW (2012) *Journal of Chemical Physics* **137,** 154701.

73. Vacha R, Rick SW, Jungwirth P, de Beer AGF, de Aguiar HB, Samson JS, & Roke S (2011) *Journal of the American Chemical Society* **133,** 10204-10210.

74. Vacha R, Marsalek O, Willard AP, Bonthuis DJ, Netz RR, & Jungwirth P (2012) *Journal of Physical Chemistry Letters* **3,** 107-111.

75. Warshel A & Weiss RM (1980) *Journal of the American Chemical Society* **102,** 6218-6226.

76. Voth GA (2006) *Accounts of Chemical Research* **39,** 143-150.

77. Petersen MK, Iyengar SS, Day TJF, & Voth GA (2004) *Journal of Physical Chemistry B* **108,** 14804-14806.

78. Swanson JMJ, Maupin CM, Chen HN, Petersen MK, Xu JC, Wu YJ, & Voth GA (2007) *Journal of Physical Chemistry B* **111,** 4300-4314.

79. Wick CD & Dang LX (2009) *Journal of Physical Chemistry A* **113,** 6356-6364.

80. Wick CD (2012) *Journal of Physical Chemistry C* **116,** 4026-4038.

81. Kuo IFW & Mundy CJ (2004) *Science* **303,** 658-660.

82. Salvador P, Curtis JE, Tobias DJ, & Jungwirth P (2003) *Physical Chemistry Chemical Physics* **5,** 3752-3757.

83. Jungwirth P, Curtis JE, & Tobias DJ (2003) *Chemical Physics Letters* **367,** 704-

710.

84. Stuart SJ & Berne BJ (1999) *Journal of Physical Chemistry A* **103,** 10300-10307.

85. Lee HS & Tuckerman ME (2009) *Journal of Physical Chemistry A* **113,** 2144-2151.

86. Baer MD, Kuo IFW, Bluhm H, & Ghosal S (2009) *Journal of Physical Chemistry B* **113,** 15843-15850.

87. Ho MH, Klein ML, & Kuo IFW (2009) *Journal of Physical Chemistry A* **113,** 2070-2074.

88. Baer MD & Mundy CJ (2011) *Journal of Physical Chemistry Letters* **2,** 1088-1093.

89. Hart EJ & Boag JW (1962) *Journal of the American Chemical Society* **84,** 4090-4095.

90. Turi L & Rossky PJ (2012) *Chemical Reviews* **dx.doi.org/10.1021/cr300144z**.

91. Herbert JM & Jacobson LD (2011) *Journal of Physical Chemistry A* **115,** 14470–14483.

92. Marsalek O, Uhlig F, Vandevondele J, & Jungwirth P (2012) *Accounts of Chemical Research* **45,** 23-32.

93. Uhlig F, Marsalek O, & P. J (2012) *Jounal of Physical Chemistry Letters* **3,** 3071–3075.

94. Larsen RE, Glover WJ, & Schwartz BJ (2010) *Science* **329,** 65-69.

95. Jacobson LD & Herbert JM (2011) *Science* **331,** 1387-d.

96. Turi L & Madarasz A (2011) *Science* **331,** 1387-c.

97. Larsen RE, Glover WJ, & Schwartz BJ (2011) *Science* **331**.

98. Siefermann KR, Liu YX, Lugovoy E, Link O, Faubel M, Buck U, Winter B, & Abel B (2010) *Nature Chemistry* **2,** 274-279.

99. Barnett RN, Landman U, Scharf D, & Jortner J (1989) *Accounts of Chemical Research* **22,** 350-357.

100. Nicolas C, Boutin A, Levy B, & Borgis D (2003) *Journal of Chemical Physics* **118,** 9689-9696.

101. Turi L, Sheu WS, & Rossky PJ (2005) *Science* **309,** 914-917.

102. Sommerfeld T, DeFusco A, & Jordan KD (2008) *Journal of Physical Chemistry A* **112,** 11021-11035.

103. Jacobson LD & Herbert JM (2010) *Journal of Chemical Physics* **133,** 154506.

104. Boero M, Parrinello M, Terakura K, Ikeshoji T, & Liew CC (2003) *Physical Review Letters* **90,** 226403.

105. Boero M (2007) *Journal of Physical Chemistry A* **111,** 12248-12256.

106. Barnett RN, Giniger R, & Cheshnovsky O (2011) *Journal of Physical Chemistry A* **115,** 7378-7391.

107. Quincke G (1861) *Ann. Phys. Chem.* **113,** 513.

108. Gilbert HW (1924) *Proceedings of the Physical Society London* **37,** 195-214.

109. Zilch LW, Maze JT, Smith JW, Ewing GE, & Jarrold MF (2008) *Journal of Physical Chemistry A* **112,** 13352-13363.

110. Graciaa A, Morel G, Saulner P, Lachaise J, & Schechter RS (1995) *Journal of Colloid and Interface Science* **172,** 131-136.

111. Najafi AS, Drelich J, Yeung A, Xu ZH, & Masliyah J (2007) *Journal of Colloid and Interface Science* **308,** 344-350.

112. Takahashi M (2005) *Journal of Physical Chemistry B* **109,** 21858-21864.

113. Marinova KG, Alargova RG, Denkov ND, Velev OD, Petsev DN, Ivanov IB, & Borwankar RP (1996) *Langmuir* **12,** 2045-2051.

114. Beattie JK & Djerdjev AM (2004) *Angewandte Chemie-International Edition* **43,** 3568-3571.

115. Beattie JK (2006) *Lab on a Chip* **6,** 1409-1411.

116. Exerowa D (1969) *Kolloid-Zeitschrift and Zeitschrift Fur Polymere* **232,** 703-&.

117. Karraker KA & Radke CJ (2002) *Advances in Colloid and Interface Science* **96,** 231-264.

118. Stubenrauch C & von Klitzing R (2003) *Journal of Physics-Condensed Matter* **15,** R1197-R1232.

119. Beattie JK, Djerdjev AM, & Warr GG (2009) *Faraday Discussion* **141,** 31-39.

120. Zimmermann R, Freudenberg U, Schweiss R, Kuttner D, & Werner C (2010) *Current Opinion in Colloid & Interface Science* **15,** 196-202.

121. Petersen PB & Saykally RJ (2008) *Chemical Physics Letters* **458,** 255-261.

122. Winter B, Faubel M, Vacha R, & Jungwirth P (2009) *Chemical Physics Letters* **474,** 241-247.

123. Ottosson N, Cwiklik L, Soderstrom J, Bjorneholm O, Ohrwall G, & Jungwirth P (2011) *Journal of Physical Chemistry Letters* **2,** 972-976.

124. Tian CS & Shen YR (2009) *Proceedings of the National Academy of Sciences of the United States of America* **106,** 15148-15153.

125. Weissenborn PK & Pugh RJ (1996) *Journal of Colloid and Interface Science* **184,** 550-563.

126. Jungwirth P (2009) *Faraday Discussions* **141,** 9-30.

127. Liu MY, Beattie JK, & Gray-Weale A (2012) *Journal of Physical Chemistry B* **116,** 8981-8988.

128. Gibbs JW (1928) *The Collected Works of J. Willard Gibbs* (Longmans, New York).

129. Kochurova NN & Rusanov AI (1981) *Journal of Colloid and Interface Science* **81,** 297-303.

130. Masamura M (2001) *Journal of Computational Chemistry* **22,** 31-37.

131. Lee HM, Tarkeshwar P, & Kim KS (2004) *Journal of Chemical Physics* **121,** 4657-4664.

132. Brodskaya E, Lyubartsev AP, & Laaksonen A (2002) *Journal of Physical Chemistry B* **106,** 6479-6487.

133. Vegiri A & Shevkunov SV (2000) *Journal of Chemical Physics* **113,** 8521-8530.

134. Vacha R, Buch V, Milet A, Devlin P, & Jungwirth P (2007) *Physical Chemistry Chemical Physics* **9,** 4736-4747.

135. Buch V, Milet A, Vacha R, Jungwirth P, & Devlin JP (2007) *Proceedings of the National Academy of Sciences of the United States of America* **104,** 7342-7347.

136. Vacha R, Horinek D, Berkowitz ML, & Jungwirth P (2008) *Physical Chemistry Chemical Physics* **10,** 4975-4980.

137. Kudin KN & Car R (2008) *Journal of the American Chemical Society* **130,** 3915-3919.

138. Vacha R, Zangi R, Engberts JBFN, & Jungwirth P (2008) *Journal of Physical Chemistry C* **112,** 7689-7692.

139. Zangi R & Engberts J (2005) *Journal of the American Chemical Society* **127,** 2272-2276.

140. Beattie JK (2009) *Chemical Physics Letters* **481,** 17-18.

141. Winter B, Faubel M, Vacha R, & Jungwirth P (2009) *Chemical Physics Letters* **481,** 19-21.

142. Gray-Weale A & Beattie JK (2009) *Physical Chemistry Chemical Physics* **11,** 10994-11005.

143. Vacha R, Horinek D, Buchner R, Winter B, & Jungwirth P (2010) *Physical Chemistry Chemical Physics* **12,** 14362-14363.

144. Gray-Weale A & Beattie JK (2010) *Physical Chemistry Chemical Physics* **12,** 14364-14366.

145. Roger K & Cabane B (2012) *Angewandte Chemie-International Edition* **51,** 5625-5628.

146. Beattie JK & Gray-Weale A (2012) *Angewandte Chemie, International Edition***,** comment submitted.

147. Jena KC, Scheu R, & Roke S (2012) *Angewandte Chemie, International Edition***,** comment submitted.

148. Mishra H, Enami S, Nielsen RJ, Steward LA, FHoffmann MR, Goddard WAI, & Colussi AJ (2012) *Proceedings of the National Academy of Sciences of the United States of America***,** doi/10.1073/pnas.1209307109.

149. Yamaguchi S, Kundu A, Sen P, & Tahara T (2012) *Journal of Chemical Physics*

137, 151101.

150. Kambhampati P, Son DH, Kee TW, & Barbara PF (2002) *Journal of Physical Chemistry A* **106,** 2374-2378.

151. Garrett BC, Dixon DA, Camaioni DM, Chipman DM, Johnson MA, Jonah CD, Kimmel GA, Miller JH, Rescigno TN, Rossky PJ*, et al.* (2005) *Chemical Reviews* **105,** 355-389.

152. Barnett RN, Landman U, Cleveland CL, & Jortner J (1987) *Physical Review Letters* **59,** 811-814.

153. Madarasz A, Rossky PJ, & Turi L (2009) *Journal of Chemical Physics* **130,** 124319.

154. Verlet JRR, Bragg AE, Kammrath A, Cheshnovsky O, & Neumark DM (2005) *Science* **307,** 93-96.

155. Ma L, Majer K, Chirot F, & von Issendorff B (2009) *Journal of Chemical Physics* **131,** 144303.

156. Marsalek O, Uhlig F, Frigato T, Schmidt B, & Jungwirth P (2010) *Physical Review Letters* **105,** 043002.

157. Madarasz A, Rossky PJ, & Turi L (2010) *Journal of Physical Chemistry A* **114,** 2331-2337.

158. Marsalek O, Uhlig F, & P. J (2010) *Journal of Physical Chemistry* **114,** 20489–20495.

159. Jacobson LD & Herbert JM (2011) *Journal of the American Chemical Society* **133,** 19889-19899.

160. Voora VK, Ding J, Sommerfeld T, & Jordan KD (2012) *Journal of Physical*

Chemistry B **DOI: 10.1021/jp306940k**.

161. Barnett RN, Giniger R, Cheshnovsky O, & Landman U (2011) *Journal of Physical Chemistry A* **115,** 7378-7391.

162. Uhlig F, Marsalek O, & P J *submitted*.

163. Sagar DM, Bain CD, & Verlet JRR (2010) *Journal of the American Chemical Society* **132,** 6917-+.

164. Asmis KR, Santambrogio G, Zhou J, Garand E, Headrick J, Goebbert D, Johnson MA, & Neumark DM (2007) *Journal of Chemical Physics* **126**.

165. Tauber MJ & Mathies RA (2003) *Journal of the American Chemical Society* **125,** 1394-1402.

166. Frigato T, VandeVondele J, Schmidt B, Schutte C, & Jungwirth P (2008) *Journal of Physical Chemistry A* **112,** 6125-6133.

167. Uhlig F, Marsalek O, & Jungwirth P (2011) *Physical Chemistry Chemical Physics* **13,** 14003-14009.

168. Markin VS & Volkov AG (2002) *Journal of Physical Chemistry B* **106,** 11810-11817.

169. Abel B, Buck U, Sobolewski AL, & Domcke W (2012) *Physical Chemistry Chemical Physics* **14,** 22-34.

170. Shreve AT, Yen TA, & Neumark DM (2010) *Chemical Physics Letters* **493,** 216-219.

171. Tang Y, Shen H, Sekiguchi K, Kurahashi N, Mizuno T, Suzuki YI, & Suzuki T (2010) *Physical Chemistry Chemical Physics* **12,** 3653-3655.

172. Buchner F, Schultz T, & Lubcke A (2012) *Physical Chemistry Chemical Physics*

14, 5837-5842.